Design and Synthesis of New Sulfur-Containing Hyperbranched Polymer and Theranostic Nanomaterials for Bimodal Imaging and Treatment of Cancer

Blaze Heckert,[§] Tuhina Banerjee,[§] Shoukath Sulthana,[§] Shuguftha Naz,[§] Riyadh Alnasser,[§] Deaven Thompson,[§] Guillaume Normand,[‡] Jan Grimm,[‡,⊥] J. Manuel Perez,[†,#] and Santimukul Santra*,[§]

[§]Department of Chemistry, Pittsburg State University, 1701 South Broadway Street, Pittsburg, Kansas 66762, United States

[†]Nanoscience Technology Center, University of Central Florida, Orlando, Florida 32826, United States

[‡]Department of Radiology and Molecular Pharmacology Program, Memorial Sloan Kettering Cancer Center, 1275 York Avenue, New York, New York 10065, United States

[⊥]Pharmacology Program and Department of Radiology, Weil Cornell Medical College, 1300 York Avenue, New York, New York 10065, United States

S *Supporting Information*

ABSTRACT: In this study, we have synthesized a new hyperbranched polyester polymer containing sulfur-pendants (HBPE-S) in the branching points. This HBPE-S polymer is composed of spherical shaped, aliphatic three-dimensional architecture with carboxylic acid groups on the surface. The presence of sulfur pendants in the polymeric cavities demonstrated an important role in the effective encapsulation of Bi-DOTA complexes ([Bi] = 5.21 μM), when compared to the previously reported polymer without sulfur pendants (HBPE, [Bi] = 1.07 $\times$ 10^{-3} μM). Higher X-ray blocking capability and excellent X-ray contrast images were obtained

from Bi-DOTA encapsulating HBPE-S polymeric nanoparticles when compared with that of HBPE nanoparticles. In addition, the HBPE-S polymer's spherical structure with amphiphilic cavities allow for the successful encapsulation of antitumor drugs and optical dyes, indicating suitable for delivery of wide-range of theranostic agents for cancer diagnosis and treatment. Therapeutic drug taxol encapsulating, folic acid decorated HBPE-S-Fol nanoparticles showed more than 80% of lung carcinoma cell death within 24 h of incubation. Cell viability and microscopic experiments also confirmed for the targeted delivery, thereby minimizing toxicity to healthy tissues. Taken together, new HBPE-S polymer and multimodal theranostic nanoplatforms were synthesized with enhanced X-ray blocking capability for the effective cancer targeting and treatment monitoring.
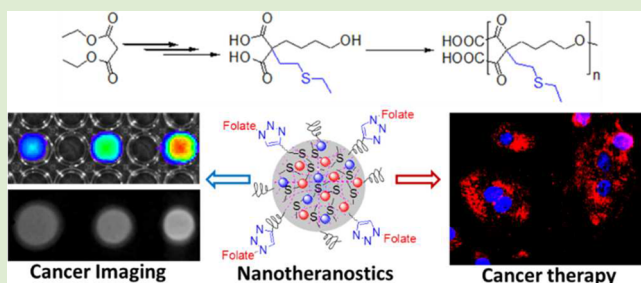
The construction of architectural polymeric materials and nanostructures such as nanospheres, nanorods, or nanowires with multimodal imaging and treatment capabilities has attracted considerable interest in the field of medicine.[1−3] Current research advances toward minimizing the toxicity of these nanostructures, which depends on the chemical nature of the nanoparticle components (lipid, polymer, inorganic compounds) and the loading dosage of the therapeutic agents.[4] For instance, inorganic nanoparticles have limited applications due to low aqueous dispersibility, long-term instability, and higher toxicity.[5−11] Therefore, the construction of new designer polymer and its biocompatible nanoparticles with minimal toxicity is important for the targeted drug delivery, imaging, and treatment of cancer.

Modern tumor imaging requires target specificity, higher resolution and three-dimensional tomography, which are difficult to meet with current single-modal and mostly nonspecific imaging agents.[12−18] X-ray computed tomography (CT) is one of the most powerful and widely used noninvasive

tissue imaging techniques, due to the deep tissue penetration capability, which displays internal anatomic structures non-invasively.[19−22] Several X-ray absorbing nanoparticle systems were developed including iodinated liposomes, polymeric micelles, inorganic nanoparticles, however, the stability and toxicity issues still need to be addressed.[23−30] In this study, we report the first example of sulfur containing hyperbranched polyester polymer and its' polymeric nanoparticles for effective encapsulation of Bi-DOTA complexes, bimodal imaging, and treatment of cancer.

Toward this end, we have synthesized a new hyperbranched polyester polymer containing multiple sulfur-pendants (HBPE-S) in the branching points (Scheme 1). The HBPE-S polymer's spherical shape with amphiphilic cavities would allow for the

Scheme 1. Stepwise Syntheses of New S-Containing Branched Monomer (5) and HBPE-S Polymer (6)

S-containing hyperbranched polyester (HBPE-S, 6)
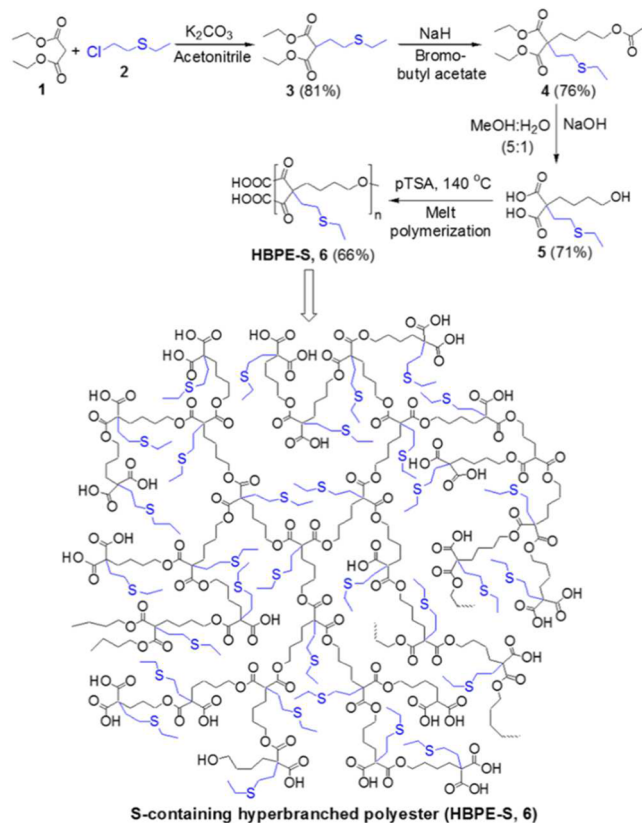
successful encapsulation of a variety of imaging and therapeutic agents for effective cancer diagnosis and treatment. Moreover, the presence of sulfur pendants in HBPE-S polymer would facilitate the effective encapsulation of higher dosage Bi-DOTA complexes (bismuth-1,4,7,10-tetraazacyclododecane-1,4,7,10-tetraacetic acid) due the intrinsic binding affinities between bismuth metal and sulfur ligand.[31,32] Thus, we hypothesized that this new HBPE-S polymer would formulate highly stable "Bi" (higher Z-number: 83) containing nanoparticles and provide better X-ray contrast comparing to iodinated (lower Z-number: 53) liposomes. It is important to note that our previously reported HBPE polymer[33,34] resulted in poor encapsulation of metal complexes. This is may be due to the absence of sulfur pendants in the structure. Together, we report the importance of developing a new sulfur-containing hyperbranched HBPE-S polymer and formulating polymeric nanostructures for the effective encapsulations of Bi-DOTA complex and DiI dye for the bimodal X-ray and optical imaging, respectively, and therapeutic drug taxol for the treatment of cancer.

Herein, we have successfully synthesized a novel aliphatic HBPE polymer with sulfur pendants for the effective loading of bismuth complexes. We hypothesized that the introduction of sulfur ligands would lead to more stable and effective encapsulation of Bi-DOTA complexes, due to its higher binding affinity for "Bi" metal (e.g., bismuth sulfide Bi_2S_3).[31,32] The synthetic protocol for this new HBPE-S polymer is illustrated in Scheme 1 (for details, see SI, Experimental Section). Importantly, the second acidic proton of compound 3 was substituted with 4-bromobutyl acetate[33,34] using NaH to synthesize the protected monomer 4. Finally, the

hydrolyzed A$_2$B monomer 5 was melt polymerized using p-toluenesulfonic acid (pTSA, 100:1 molar ratio) as catalyst, under reduced pressure and at 150 °C.[33] The rate of polymerization and molecular weight of the polymer were controlled by varying reaction time under vacuum (0.2 mm/Hg). We observed that low molecular weight oligomers were synthesized without applying vacuum (SI, Table S1). The resulting HBPE-S polymer 6 was purified using mixed-solvent precipitation method where the polymer was precipitated in methanol from DMSO solution. The successful syntheses of monomers and HBPE-S polymer were indicated by ¹H NMR (Figure 1), FT-IR (SI, Figure S1) and thermogravimetric
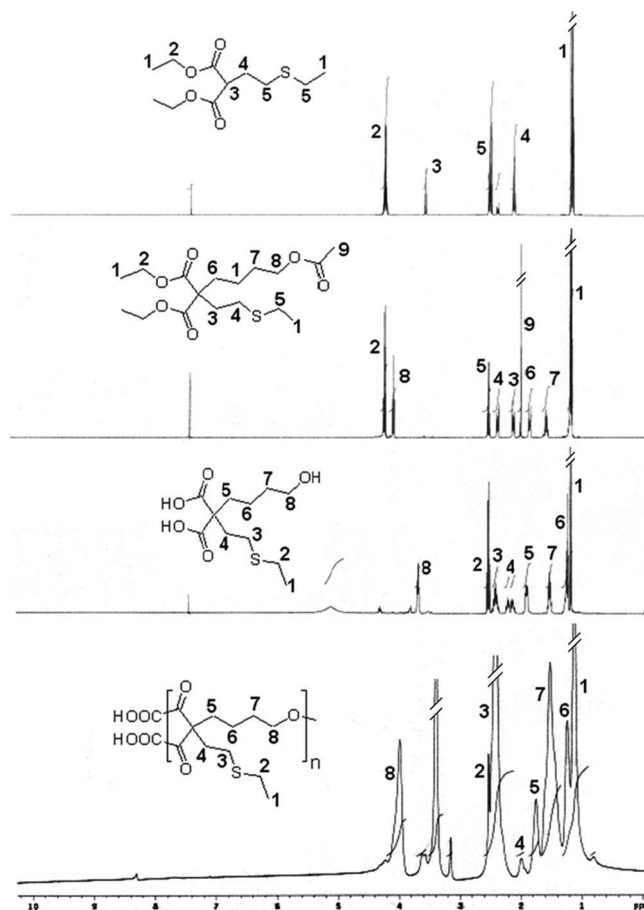

Figure 1. ¹H NMR spectra of the synthesized new functional monomers and the S-containing HBPE-S polyester (6).

analysis. The molecular weight of the HBPE-S polymer was calculated using size exclusion chromatography (SEC) and indicate for the synthesis of higher molecular weight polymer (M_w = 38000, PD = 1.86), as showed in Figure 2A.

Next, HBPE-S polymer was used for the one-pot formulation of cargos-encapsulating polymeric nanoparticles (PNPs) using solvent diffusion method (Figure 2, see SI, Experimental Section).[35,36] We have selected DiI dye (5 μg/μL) for optical imaging, Bi-DOTA complex (30 μg/μL) for enhanced X-ray attenuation and therapeutic drug taxol (1 μg/μL) for treatment. Dynamic light scattering method (DLS) was used for the determination of size of this carboxylated PNPs 7, and the overall diameter was found to be 82 ± 2 nm (Figure 2B). The presence of free carboxylic acid groups on HBPE-S PNPs was confirmed by measuring ζ-potential (−45 mV, SI, Figure S2).
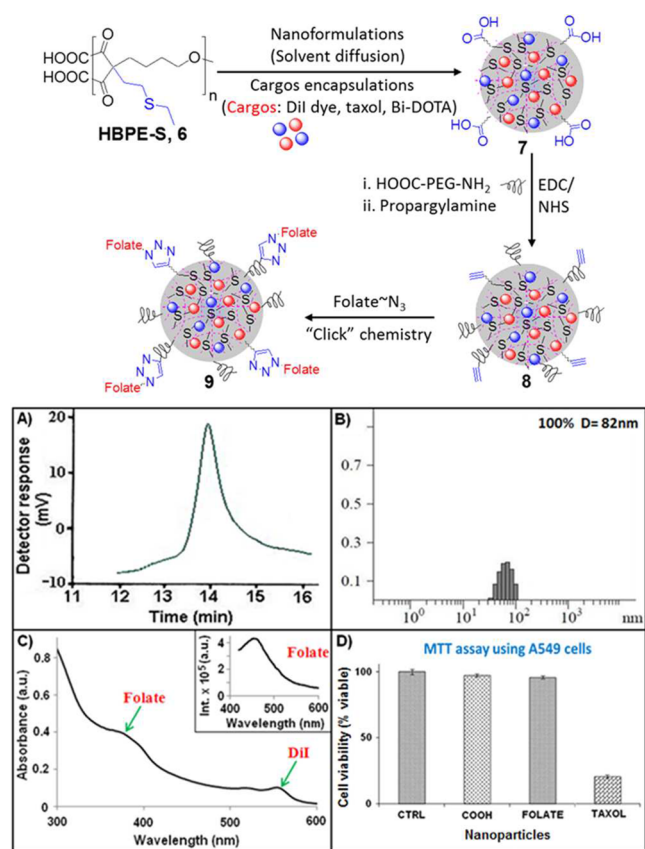
Figure 2. Schematic representation of nanoformulation, and characterization of HBPE-S polymer and functional PNPs. (A) GPC chromatogram of HBPE-S polymer **6**; (B) DLS histogram of PNPs **7**; (C) UV−vis spectrum of PNPs **9** showing the presence of folic acid (λ_{abs} = 380 nm) and DiI dye (λ_{abs} = 554 nm); Inset: Fluorescence spectrum confirming the presence of folic acid (λ_{em} = 452 nm); (D) Evaluation of cytotoxicity of functional PNPs using MTT assay. Average values of three measurements are depicted ± standard error. 1× PBS solution was used for the control cells treatment.

In order to facilitate targeted Non-Small-Cell Lung Cancer (NSCLC) treatment and retention in blood circulation, we have used these surface carboxylic acids for the conjugation of folate-receptor targeting folic acid and polyethylene glycol polymer (H$_2$N-PEG-COOH, M_w = 617.17) using "Click" chemistry and standard EDC/NHS-based carbodiimide chemistry, respectively.[37−40] Functional HBPE-S PNPs (**7**−**9**, Figure 2) were purified using PD-10 columns and dialyzed (MWCO 6−8K) against PBS solution (pH = 7.4). Nanoparticles were found to be stable in PBS (pH = 7.4) and in serum for longer periods of time, as no significant agglomeration (by DLS) or quenching in fluorescent emission were observed with time (SI, Table S2). The effect of PEGylation was reflected in the change in overall diameter (D = 85 nm, SI, Figure S3) of PNPs. The effective conjugation of folic acid was verified by spectrophotometric experiments as shown in Figure 2C. The presence of absorbance maximum λ_{abs} at 380 nm and fluorescence emission λ_{em} at 452 nm (inset, Figure 2C) confirmed for the successful conjugation of folic acid. Molecular encapsulation of DiI dye and taxol (encapsulation efficiency, EE$_{DiI}$ = 67% and EE$_{taxol}$ = 73%) were confirmed by UV−vis (DiI dye: λ_{abs} at 554 nm) and fluorescence (DiI dye: λ_{em} at 572 nm, SI, Table S2; taxol: λ_{em} at 370 nm, SI, Figure S4) spectroscopic methods. All these

functionalized PNPs were further confirmed by DLS and ζ-potential analyses (SI, Table S2 and Figure S2).

To evaluate the potential X-ray blocking properties of our Bi-DOTA complex-encapsulating HBPE-S NPs (**9**) and to compare that with Bi-DOTA complex-encapsulating HBPE NPs, these PNPs were first characterized using ICP-MS spectrometer. Results showed that the HBPE-S PNPs (**9**) contain more Bi-DOTA complex ([Bi] = 5.21 μmol) than HBPE PNPs ([Bi] = 1.07 × 10^{-3} μmol). These results directly acknowledge our hypothesis and further prove for the affinity of "Bi" atoms toward "S" atoms. Various concentrations of Bi-HBPE-S NPs were prepared and taken in a 96-well plate for optical (Xenogen IVIS optical imaging system) and X-ray imaging (Concorde Microsystem's X-ray instrument). With increased concentrations of Bi-HBPE-S NPs (1, 2, 3, and 5 mg/mL), higher fluorescence intensity (Figure 3A) and X-ray
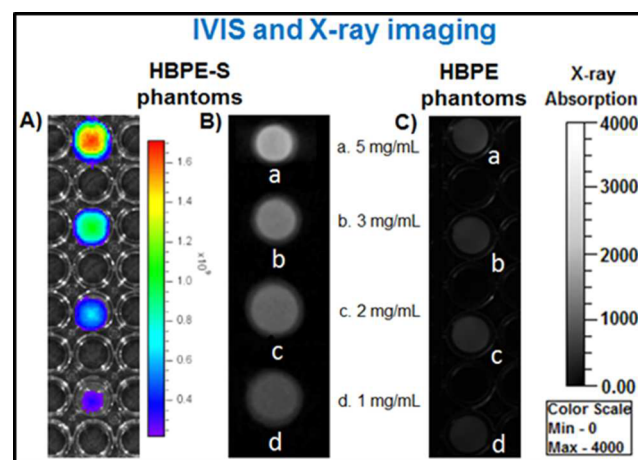

Figure 3. Bimodal (optical and X-ray) imaging of PNPs phantoms (1−5 mg/mL). (A) IVIS and X-ray images of (B) HBPE-S NPs (**9**) and (C) corresponding HBPE NPs phantoms.

contrasts were observed (Figure 3B). In contrast, due to the lack of efficient Bi-DOTA encapsulation, we have not observed any noticeable X-ray contrast from Bi-HBPE NPs phantoms (Figure 3C). These results indicate the importance of new HBPE-S polymer with sulfur pendants in the cavities. It is important to note that our Bi-HBPE-S NPs phantoms have comparable X-ray attenuation properties with clinically approved Omnipaque solutions (SI, Figure S5). Taken together, these results indicated that the new HBPE-S polymer holds promise for effective Bi-DOTA complex encapsulations and X-ray imaging, and indicative of its importance in the field of macromolecular science.

The effective release studies of the encapsulating drug and imaging agents in HBPE-S PNPs (**9**) are important for potential therapeutic applications. We have designed experiments with esterase enzyme (from porcine liver) and at acidic pH (pH = 6.0) using the dynamic dialysis technique.[37] In particular, the low-pH condition was used to mimic tumor cell's intracellular acidic microenvironment. Results showed for a time-dependent release of taxol drug (Figure 4A,B) and within 6−8 h of incubation either in the presence of esterase enzyme or acidic pH. Faster release was observed in acidic pH when compared with esterase enzyme. This is attributed to the faster acidic hydrolysis of polymer backbone's ester linkages and subsequent release of drug. We further assume that upon polymer backbone degradation, the optical and X-ray contrast
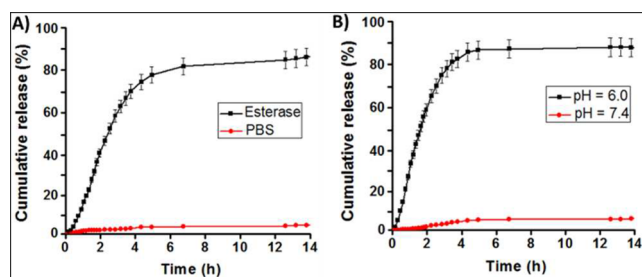
Figure 4. Evaluation of drug release profiles for taxol encapsulating HBPE-S NPs (**9**) using dialysis method at 37 °C. Within a course of time, taxol drug was released when incubated with (A) esterase enzyme and (B) acidic buffered solution. No significant release of drug was found in physiological pH (red lines, A, B).

A549 cells for 24 h before visualized using fluorescence microscope. Results showed minimal internalizations for carboxylated NPs (Figure 5A−C), as expected due to the
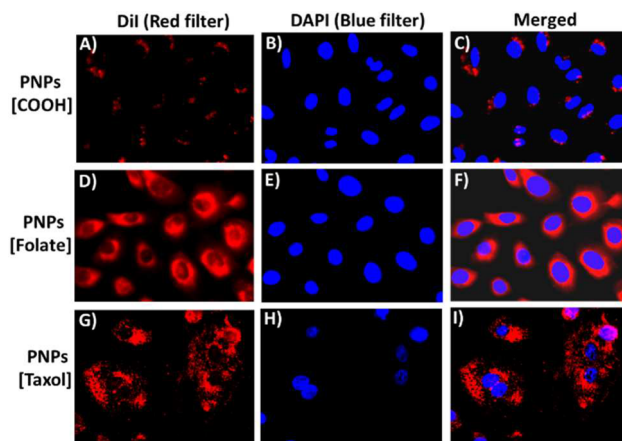

Figure 5. Assessment of HBPE-S PNP's cellular uptake and cytotoxicity using fluorescence microscopy. A-C) Minimal internalization was observed with carboxylated NPs (**7**), whereas (D−F) enhanced internalization was observed with folate NPs. (G−I) A549 cells were incubated with taxol encapsulating folate NPs (**9**), leading to mitotic arrest and cell death. Nuclei stained with DAPI dye (blue).

agents will be released, simultaneously. On the other hand, minimum amount of drug was released under physiological pH and in serum conditions, which indicated for stability in physiological conditions. Additionally, to mimic real in vivo conditions, the PNPs were incubated with 55% plasma proteins before subjected to drug release experiments at pH 6.0. The protein corona-coated PNPs were found to be stable with little bigger in size (94 nm, SI, Figure S6) and as expected, a slower rate of drug release was observed and reported in SI, Figure S7. Together, these results indicated that our HBPE-S nanoparticles would be ideal for in vivo drug delivery applications.

To assess HBPE-S PNP's potential cytotoxicity and to determine the ability for targeted drug delivery, we have performed MTT assay. In experiments, the folate receptor positive non-small-cell lung cancer (NSCLC) cells[41,42] were seeded in a 96-well plate and various functional HBPE-S NPs (2.5 mM) were incubated for 24 h (Figure 2D). The carboxylated PNPs (COOH, **7**) showed minimal toxicity due to the lack of internalizations, and the folate PNPs (FOLATE, **9**, without taxol drug) also showed very minimal toxicity (around 5% cell death) to NSCLC. These results indicated that the formulated PNPs are suitable for drug delivery and showed little extent of toxicity may be due to the presence of Bi-DOTA complex within the PNP's cavity. However, more than 80% cell death was observed within 24 h, when incubated with taxol[43−45] encapsulating HBPE-S PNPs (TAXOL, **9**, Figure 2D). To mimic in vivo conditions, similar experiments were performed incubating protein corona-coated PNPs with serum-starved A549 cells, and more than 55% cell death was observed after 24 h of incubation (SI, Figure S8). These results confirmed that the therapeutic drug taxol's antitumor activity is preserved irrespective of its encapsulation, successful drug delivery and treatment by HBPE-S NPs. In another set of experiments, rat cardiomyocytes (H9c2, FR−)[46] cells were incubated with taxol carrying PNPs (**9**, SI, Figure S9) and showed minimal cytotoxicity after 24 h of incubation. This result further indicated for folate receptor-mediated internalizations and targeted drug delivery. In conclusion, these findings suggested that the HBPE-S nanoparticles were capable of targeted delivery of anticancer drug and imaging agents specifically to the tumors in order to prevent side effects to the nontransformed cells and normal tissues.

To further explore the potential targeted therapeutic applications, we evaluated surface-charge and functionality-dependent cellular internalizations and cytotoxicity of HBPE-S NPs. In these experiments, carboxylated (**7**, COOH) or folate-conjugated (**9**, Folate) NPs (2.5 mM) were incubated with

enhanced permeability and retention (EPR) effect and lack of effective folate-receptor mediated internalizations. However, enhanced internalizations were observed from folate NPs with no drug (Figure 5D−F), further indicating for the receptor-mediated internalizations. In addition, no significant internalization of folate NPs was observed when lung cancer cells (FR+) were preincubated with excess of folic acid (competition assay, SI, Figure S10) and in studies using H9c2 cardiomyocyte cells (FR−, SI, Figure S11). These results corroborated for folate receptor-mediated internalizations. Next, we investigated for the intracellular uptake of taxol-encapsulating folate-conjugated PNPs (**9**, Taxol) in NSCLC and treatment. Upon 24 h of incubation, mitotic arrest was observed, leading to changes in cellular morphology and cell death (Figure 5G−I). These results indicate that the novel folate-conjugating HBPE-S NPs can deliver theranostic agents specifically to folate receptor-expressing tumors, while visualizing drug delivery and cancer treatment.

In conclusion, we have developed a new hyperbranched polyester polymer with sulfur pendants (HBPE-S) in each branching point. The presence of sulfur pendants facilitated higher concentration loading of bismuth complexes (Bi-DOTA), when compared with the HBPE polymer without sulfur pendants. ICP-MS results showed the presence of higher concentration bismuth ([Bi] = 5.21 μM) and observed enhanced X-ray attenuation from HBPE-S NPs when compared with HBPE NPs ([Bi] = 1.07 × 10^{-3} μM). In addition, the synthesized novel HBPE-S NPs were highly efficient in targeted delivery of therapeutic drugs to NSCLC cells, while minimizing potential toxicity to healthy tissues. Taken together, we have developed a new sulfur-containing hyperbranched polymer and functional nanostructures capable of (i) encapsulating Bi-DOTA complex in higher concentrations for enhanced X-ray contrast, (ii) delivering of anticancer drugs specifically to tumor, and (iii) multiparametric (optical and X-ray) imaging of drug homing and monitoring of treatment. This result brings an

important piece of information for the structure and property relationships and adds a new drug delivery system for the effective X-ray and optical imaging and treatment of cancer. Further work, including an in vivo demonstration of X-ray contrast and targeted drug delivery, are currently under investigation.

■ ASSOCIATED CONTENT

Ⓢ Supporting Information

The Supporting Information is available free of charge on the ACS Publications website at DOI: 10.1021/acsmacrolett.7b00008.

> Synthesis and characterizations of monomers and polymer, nanoparticle characterizations, FT-IR spectra, ζ-potential studies, receptor-mediated cellular internalizations, cytotoxicity, and IVIS imaging (PDF)

■ AUTHOR INFORMATION

Corresponding Author

*E-mail: ssantra@pittstate.edu.

ORCID Ⓘ

Santimukul Santra: 0000-0002-5047-5245

Present Address

#Biomedical Imaging Research Institute, Department of Biomedical Sciences and Department of Neurosurgery, Cedars Sinai Medical Center, 127 San Vicente Blvd, Los Angeles CA, 90048, United States.

Notes

The authors declare no competing financial interest.

■ ACKNOWLEDGMENTS

■ REFERENCES

(1) Whitesides, G. M.; Mathias, J. P.; Seto, C. T. *Science* **1991**, *254*, 1312−1319.

(2) Whitesides, G. M.; Grzybowski, B. *Science* **2002**, *295*, 2418−2421.

(3) Zhang, S. *Nat. Biotechnol.* **2003**, *21*, 1171−1178.

(4) Attia, M. F.; Anton, N.; Chiper, M.; Akasov, R.; Anton, H.; Messaddeq, N.; Fournel, S.; Klymchenko, A. S.; Mely, Y.; Vandamme, T. F. *ACS Nano* **2014**, *8*, 10537−10550.

(5) Oh, M. H.; Lee, N.; Kim, H.; Park, S. P.; Piao, Y.; Lee, J.; Jun, S. W.; Moon, W. K.; Choi, S. H.; Hyeon, T. *J. Am. Chem. Soc.* **2011**, *133*, 5508−5515.

(6) Kattumuri, V.; Katti, K.; Bhaskaran, S.; Boote, E. J.; Casteel, S. W.; Fent, G. M.; Robertson, D. J.; Chandrasekhar, M.; Kannan, R.; Katti, K. V. *Small* **2007**, *3*, 333−341.

(7) Hainfeld, J. F.; Slatkin, D. N.; Focella, T. M.; Smilowitz, H. M. *Br. J. Radiol.* **2006**, *79*, 248−253.

(8) Kim, D.; Park, S.; Lee, J. H.; Jeong, Y. Y.; Jon, S. *J. Am. Chem. Soc.* **2007**, *129*, 7661−7665.

(9) Eck, W.; Nicholson, A. I.; Zentgraf, H.; Semmler, W.; Bartling, S. *Nano Lett.* **2010**, *10*, 2318−2322.

(10) Chanda, N.; Kattumuri, V.; Shukla, R.; Zambre, A.; Katti, K.; Upendran, A.; Kulkarni, R. R.; Kan, P.; Fent, G. M.; Casteel, S. W.;

Smith, C. J.; Boote, E.; Robertson, J. D.; Cutler, C.; Lever, J. R.; Katti, K. V.; Kannan, R. *Proc. Natl. Acad. Sci. U. S. A.* **2010**, *107*, 8760−8765.

(11) Rabin, O.; Perez, J. M.; Grimm, J.; Wojtkiewicz, G.; Weissleder, R. *Nat. Mater.* **2006**, *5*, 118−122.

(12) Cheon, J.; Lee, J. H. *Acc. Chem. Res.* **2008**, *41*, 1630−1640.

(13) Zhao, J.; Song, S.; Zhong, M.; Li, C. *ACS Macro Lett.* **2012**, *1*, 150−153.

(14) Nayak, S.; Lee, H.; Chmielewski, J.; Lyon, L. A. *J. Am. Chem. Soc.* **2004**, *126*, 10258−10259.

(15) Kim, C. K.; Ghosh, P.; Pagliuca, C.; Zhu, Z. J.; Menichetti, S.; Rotello, V. M. *J. Am. Chem. Soc.* **2009**, *131*, 1360−1361.

(16) You, C. C.; Miranda, O. R.; Gider, B.; Ghosh, P. S.; Kim, I. B.; Erdogan, B.; Krovi, S. A.; Bunz, U. H.; Rotello, V. M. *Nat. Nanotechnol.* **2007**, *2*, 318−323.

(17) Singh, M. P.; Atkins, T. M.; Muthuswamy, E.; Kamali, S.; Tu, C.; Louie, A. Y.; Kauzlarich, S. M. *ACS Nano* **2012**, *6*, 5596−5604.

(18) Kim, T.; Momin, E.; Choi, J.; Yuan, K.; Zaidi, H.; Kim, J.; Park, M.; Lee, N.; McMahon, M. T. *J. Am. Chem. Soc.* **2011**, *133*, 2955−2961.

(19) Liu, Y.; Ai, K.; Lu, L. *Acc. Chem. Res.* **2012**, *45*, 1817−1827.

(20) Beck, T.; Sheldrick, G. M. *Acta Crystallogr., Sect. E: Struct. Rep. Online* **2008**, *64*, o1286.

(21) Schwenzer, N. F.; Springer, F.; Schraml, C.; Stefan, N.; Machann, J.; Schick, F. *J. Hepatol.* **2009**, *51*, 433−445.

(22) deKrafft, K. E.; Xie, Z.; Cao, G.; Tran, S.; Ma, L.; Zhou, O. Z.; Lin, W. *Angew. Chem., Int. Ed.* **2009**, *48*, 9901−9904.

(23) Li, X.; Anton, N.; Zuber, G.; Vandamme, T. *Adv. Drug Delivery Rev.* **2014**, *76*, 116−133.

(24) Anton, N.; Vandamme, T. F. *Pharm. Res.* **2014**, *31*, 20−34.

(25) Jakhmola, A.; Anton, N.; Vandamme, T. F. *Adv. Healthcare Mater.* **2012**, *1*, 413−431.

(26) Li, X.; Anton, N.; Zuber, G.; Zhao, M.; Messaddeq, N.; Hallouard, F.; Fessi, H.; Vandamme, T. F. *Biomaterials* **2013**, *34*, 481−491.

(27) Jakhmola, A.; Anton, N.; Anton, H.; Messaddeq, N.; Hallouard, F.; Klymchenko, A.; Mely, Y.; Vandamme, T. F. *Biomaterials* **2014**, *35*, 2981−2986.

(28) Iyer, A. S.; Lyon, L. A. *Angew. Chem., Int. Ed.* **2009**, *48*, 4562−4566.

(29) Nayak, S.; Lyon, L. A. *Angew. Chem., Int. Ed.* **2005**, *44*, 7686−7708.

(30) Boal, A. K.; Ilhan, F.; DeRouchey, J. E.; Thurn-Albrecht, T.; Russell, T. P.; Rotello, V. M. *Nature* **2000**, *404*, 746−748.

(31) Tu, C.; Osborne, E. A.; Louie, A. Y. *Ann. Biomed. Eng.* **2011**, *39*, 1335−1348.

(32) Major, J. L.; Parigi, G.; Luchinat, C.; Meade, T. J. *Proc. Natl. Acad. Sci. U. S. A.* **2007**, *104*, 13881−13886.

(33) Santra, S.; Kaittanis, C.; Perez, J. M. *Langmuir* **2010**, *26*, 5364−5373.

(34) Santra, S.; Kumar, A. *Chem. Commun.* **2004**, 2126.

(35) McCarthy, J. R.; Perez, J. M.; Bruckner, C.; Weissleder, R. *Nano Lett.* **2005**, *5*, 2552−2556.

(36) Packard, B. S.; Wolf, D. E. *Biochemistry* **1985**, *24*, 5176−5181.

(37) Santra, S.; Kaittanis, C.; Grimm, J.; Perez, J. M. *Small* **2009**, *5*, 1862−1868.

(38) Sun, E. Y.; Josephson, L.; Weissleder, R. *Mol. Imaging* **2006**, *5*, 122−128.

(39) Bachovchin, D. A.; Brown, S. J.; Rosen, H.; Cravatt, B. F. *Nat. Biotechnol.* **2009**, *27*, 387−394.

(40) Kolb, H. C.; Finn, M. G.; Sharpless, K. B. *Angew. Chem., Int. Ed.* **2001**, *40*, 2004−2021.

(41) Yuan, H.; Miao, J.; Du, Y. Z.; You, J.; Hu, F. Q.; Zeng, S. *Int. J. Pharm.* **2008**, *348*, 137−145.

(42) Nelson, M. E.; Loktionova, N. A.; Pegg, A. E.; Moschel, R. C. *J. Med. Chem.* **2004**, *47*, 3887−3891.

(43) Davis, M. E.; Chen, Z. G.; Shin, D. M. *Nat. Rev. Drug Discovery* **2008**, *7*, 771−782.

(44) Fonseca, C.; Simoes, S.; Gaspar, R. *J. Controlled Release* **2002**, *83*, 273−286.

(45) Gupte, A.; Ciftci, K. *Int. J. Pharm.* **2004**, *276*, 93−106.
(46) Parker, N.; Turk, M. J.; Westrick, E.; Lewis, J. D.; Low, P. S.; Leamon, C. P. *Anal. Biochem.* **2005**, *338*, 284−293.